Thermal slip for liquids at rough solid surfaces

Chengbin Zhang,[1] Yongping Chen,[1,*] and G. P. Peterson[2]
[1]*Key Laboratory of Energy Thermal Conversion and Control of Ministry of Education, School of Energy and Environment, Southeast University, Nanjing, Jiangsu 210096, PR China*
[2]*George W. Woodruff School of Mechanical Engineering, Georgia Institute of Technology, Atlanta, Georgia 30332-0325, USA*
(Received 13 July 2012; revised manuscript received 8 January 2014; published 18 June 2014)

Molecular dynamics simulation is used to examine the thermal slip of liquids at rough solid surfaces as characterized by fractal Cantor structures. The temperature profiles, potential energy distributions, thermal slip, and interfacial thermal resistance are investigated and evaluated for a variety of surface topographies. In addition, the effects of liquid-solid interaction, surface stiffness, and boundary condition on thermal slip length are presented. Our results indicate that the presence of roughness expands the low potential energy regions in adjacent liquids, enhances the energy transfer at liquid-solid interface, and decreases the thermal slip. Interestingly, the thermal slip length and thermal resistance for liquids in contact with solid surfaces depends not only on the statistical roughness height, but also on the fractal dimension (i.e., topographical spectrum).

DOI: 10.1103/PhysRevE.89.062407 PACS number(s): 68.08.−p, 44.20.+b, 47.61.−k, 47.85.−g

I. INTRODUCTION

Thermal slip at a solid surface, by its very nature, is dominated by the interactions occurring at the interface, in relation to the nature of the fluid [1–4]. While a "perfectly smooth surface" can serve as an idealized model, the surface topography is one of the most important interfacial properties [5] to be considered in exploration of the thermal slip phenomenon. Moreover, modeling the heat transfer of liquids confined in a space is typically primarily based upon the thermal boundary that exists at the liquid-solid interface. The characteristics at the thermal boundary cannot typically be deduced from the energy conservation equations alone and is also difficult to determine experimentally. For these reasons, it is of particular importance to be able to better understand the fundamental behavior and characteristics of the thermal slip occurring at the interface of liquids and rough-solid surfaces.

The thermal slip at the boundary, which is also called temperature jump phenomena, arises when the heat flows across the liquid-solid interface. Generally the degree of thermal slip can be identified by thermal slip length, which is also known as the Kapitza length $l_s = \Delta T_i/(\partial T/\partial n)|_{\mathrm{w}}$ [where ΔT_i is the interfacial temperature jump and $(\partial T/\partial n)|_{\mathrm{w}}$ is the temperature gradient of a liquid at the wall surface]. Historically, molecular dynamics simulation has been used to examine the thermal slip at liquid-solid interfaces [2,6–8], and in so doing to probe the microscopic thermal behavior of liquids at atomically smooth solid surfaces. However, in reality solid surfaces, even at the atomic or molecular length scales, are never "perfectly smooth." The liquid-solid interaction at solid interfaces is greatly affected by the geometric structure of the rough surface. Wang and Keblinski [9] investigated the role of wetting and regular nanoscale roughness on thermal conductance at liquid-solid interfaces. However, how the detailed nature of the surface roughness, including variations in statistical roughness height and topographical spectrum, affect the thermal slip is still not well understood.

Previous investigations have observed that the surface roughness profiles at all magnifications appear quite qualitatively similar in structure and demonstrate the multiscale property [10–12]. These rough surface profiles nearly always follow power laws and hence, create a self-affine property. In view of the feature of scale invariance and geometric self-affinity, fractal characterization of the geometric structure of rough surfaces has been applied to explore and examine the solid-solid interfacial thermal resistance using Fourier's law [13], heat and fluid flow in microchannel by computational fluid dynamics simulation [14,15], and viscous slip flows past solid interfaces through molecular dynamics simulation [16]. The investigation of liquid slip flow at rough solid surfaces indicates that the viscous dissipation as a liquid flows past surface irregularities, reduces the slip velocity at the solid interface, and increases with respect to the roughness height or fractal dimension can lead to a reduction of velocity slip at the boundary [16].

Differing from liquid flow past a solid surface [17,18], the thermal conductance at the liquid-solid interface occurs without the aid of an external driving force. As an analogous physical phenomenon, it is not known whether the thermal slip at the solid surface induced by the detailed nature of the surface roughness retains the same trend as the velocity slip at the rough liquid-solid interface. In addition, the effect of the surface topography on the potential energy distribution in adjacent liquids and the effect of the thermal vibration of the wall particles on the thermal slip have not been adequately investigated. In particular, little attention has been paid to relating the surface topography to the thermal slip, especially the topographical spectrum as characterized by fractal dimension. Here we conduct a molecular dynamics simulation to investigate the thermal conductance at rough solid surfaces as characterized by fractal geometry, in an attempt to elucidate the thermal slip for liquids at rough solid surfaces.

II. FRACTAL CHARACTERIZATION OF A ROUGH SURFACE

In this paper we introduce the fractal Cantor structures to characterize the rough surface topography. Within the

*Corresponding author: ypchen@seu.edu.cn

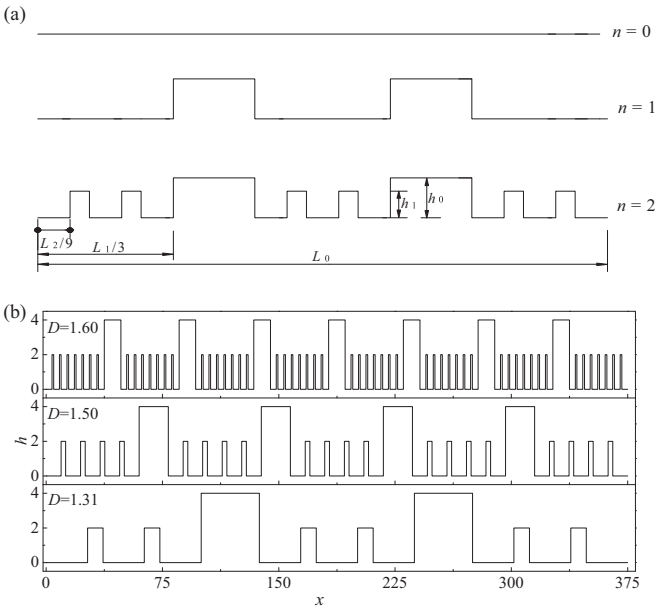

FIG. 1. Fractal characterization of rough surface: (a) Generation of Cantor set surface profile ($s = 3$). (b) Rough surface constructed from fractal Cantor structures ($\delta = 2$).

framework of the model for the fractal Cantor structure, each asperity is treated as a simple one-dimensional axially column. In this characterization, the fractal Cantor structure construct can be achieved by joining the segments at successive stages of the Cantor set [10,14], as shown in Fig. 1(a). For the Cantor set surface profile, the horizontal length and the salient height of the $(n + 1)$th level of the Cantor set surface are

$$L_{n+1} = \left(\frac{1}{f_x}\right) L_n = \left(\frac{1}{f_x}\right)^{n+1} L_0, \tag{1}$$

$$h_{n+1} = \left(\frac{1}{f_y}\right) h_n = \left(\frac{1}{f_y}\right)^{n+1} h_0, \tag{2}$$

where L_0 is the length of the surface profile, h_0 is the zero level roughness height, and f_x, f_y are the proportional coefficients, in which $h_0 = 2\delta$ (δ is the root mean square height) [10]. The self-affine fractal dimension for the Cantor set surface can be related to the parameters f_x, f_y and s [10],

$$D = 1 - \frac{\ln f_y}{\ln s f_x} + \frac{\ln s}{\ln s f_x} \quad (1 < D < 2), \tag{3}$$

where s corresponds to the number of asperities on a repeating segment and provides a spatial distribution of the asperities. As previously indicated [10,14], once D and δ for a real rough surface are given, the parameters f_x, f_y and s are determined, and then the Cantor set surface can be generated using Eqs. (1) and (2). In this investigation it is assumed that $f_x = 5/4$, $f_y = 2$, which generate a Cantor set surface with fractal dimensions of $D = 1.31$, 1.43, 1.50, 1.55, 1.60 corresponding to $s = 3$, 4, 5, 6, 8, respectively.

Figure 1(b) presents three of these typical Cantor set surface profiles. As illustrated, although the statistical roughness height is the same, the spatial distributions for the rough surfaces are more frequently varied for larger self-affine fractal dimensions.

III. MATHEMATICAL MODEL

To investigate the thermal behavior occurring at liquid-solid interface, the molecular dynamics model and continuous heat transfer model are available in the literature. Kim *et al.* [19] investigated the viscous heating of shear driven liquid flows in nanochannel by molecular dynamics (MD) simulations and their results indicate that temperature profiles predicted by the continuum model subjected to the proposed temperature jump model agree with the MD simulation results. Sun *et al.* [20] used a hybrid simulation method (combination of molecular dynamics method and finite volume method) to investigate the velocity profile, temperature profile, slip length, and Kapitza length of Poiseuille flows in a rough nanochannel.

In this investigation we focus on the thermal slip for liquids at rough solid surfaces via molecular dynamics simulation, especially to elucidate how surface topography affects thermal slip behavior at liquid-solid interface. Lepri *et al.* [21] reviewed the thermal conduction in classical low-dimensional lattices and discussed the role of lattice dimensionality on the breakdown of Fourier's law. Undoubtedly, three-dimensional (3D) molecular dynamics simulation is more capable of probing the microscopic thermal behavior at the liquid-solid interface, but it greatly increases the computation cost due to that very long nanochannel length is required to construct the fractal characteristics of rough surface. In the simulation, the dimension of the computational domain along the nanochannel length is assumed to be $L_x = 375\sigma$. In fact, the two-dimensional (2D) molecular dynamics simulation is capable of elucidating how surface topography affects thermal slip behavior at the liquid-solid interface, including statistical roughness height and topographical irregularity. And the 2D molecular dynamics simulation is more efficient in computation. Therefore, we perform a two-dimensional molecular dynamics simulation of the thermal conductance confined in a nanochannel so as to investigate the thermal slip at a rough liquid-solid interface, in which the constant temperatures are imposed at the upper and lower solid wall. As illustrated in Fig. 2, the liquids are confined between two parallel atomistic solid walls. The structures of the smooth upper wall and rough lower wall are both taken into consideration, and the rough solid wall is characterized by fractal Cantor structures. The dimensions of the computational domain in the x and y directions are $L_x \times L_y = 375\sigma \times 29\sigma$, and the rough nanochannel has a height $H = 25\sigma$.

The interatomic interactions are modeled by the Lennard-Jones (LJ) potentials [22]

$$u^{lj}(r) = 4\varepsilon\left[\left(\frac{\sigma}{r}\right)^{12} - \left(\frac{\sigma}{r}\right)^{6}\right], \tag{4}$$

where r is the interatomic spacing, and ε and σ are the energy and length scales, respectively. It is important to note that the interatomic interactions contain the liquid-liquid, liquid-solid, and solid-solid interactions. The cutoff distances for all three of these interactions are set at $r_c = 2.5\sigma$ so as to reduce the computation time. In all cases, the strength of the solid-solid interaction ε_{ss} is 50 times that of the liquid-liquid interaction

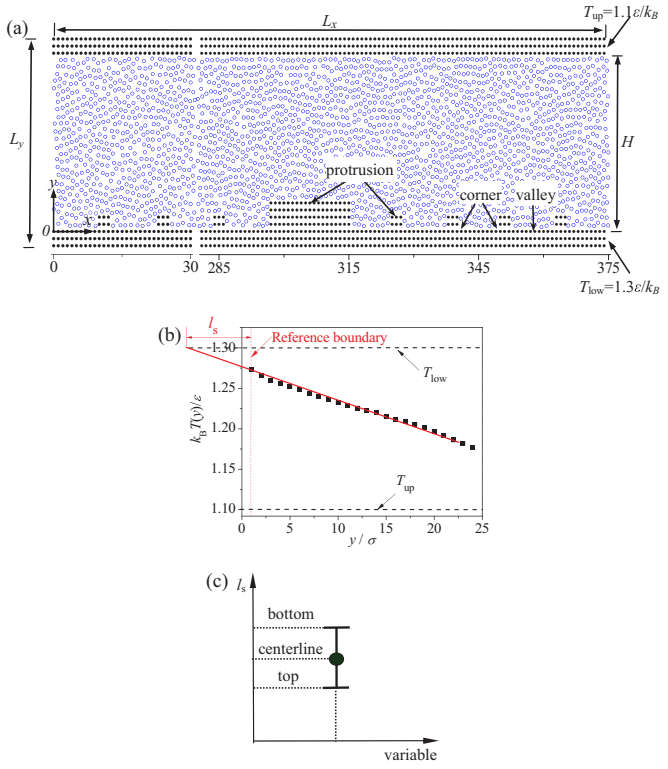

FIG. 2. (Color online) Thermal slip at a rough surface: (a) Schematic of thermal conductance of liquid in a rough nanochannel, (b) definition of thermal slip length, and (c) label for uncertainty range of thermal slip length.

ε_{ll}, in which ε_{ll} is taken as the reference energy and is equal to unity (from now on ε_{ll} will be referred to as ε); the parameters of the length scale σ are the same for all interactions.

In the simulation, a periodic boundary condition is imposed in the direction parallel to the walls. The liquid density is fixed at $\rho_l\,\sigma^3 = 0.8$, and the density of the solid wall is $\rho_s = 1.25\rho_l$. The wall atoms are tethered to their initial position by applying a spring force $\boldsymbol{F} = -K[\boldsymbol{r}(t) - \boldsymbol{r}_{eq}]$, where $\boldsymbol{r}(t)$ is the vector position of a wall atom at time t, $\boldsymbol{r}_{eq}$ is the initial position vector, and K is the spring constant which characterizes the wall stiffness. Note that the solid atoms tethered to their initial positions are sufficient to ensure the solid atoms fluctuate about the specified initial positions, thus preventing the solid atoms from ever leaving the computational domain. As a pivotal wall parameter, the stiffness correlates the wall model and real materials and determines the physical properties of the solid wall [23]. In this investigation, $K = 100\varepsilon\sigma^{-2}$ and $K = 1000\varepsilon\sigma^{-2}$ were assumed to compare the effect of wall stiffness on thermal slip at the rough solid surface. These two values are in accordance with typical magnitudes used in previous molecular dynamics simulations [23–25].

A standard molecular dynamics technique is applied and Newton's equations of motion are integrated using the Verlet algorithm to evaluate the atomic trajectories. The simulation for the system is of time step $\Delta t = 0.005\tau$, where τ represents the characteristic time of the Lennard-Jones potential. The initial structure is equilibrated in microcanonical ensemble (nve) for 1 million time steps. After equilibration, the Nose-Hoover thermostat was applied to the solid wall atoms, which were assigned a constant temperature $T_{up} = 1.1\varepsilon/k_B$ to the smooth upper wall and another constant temperature $T_{low} = 1.3\varepsilon/k_B$ to the rough lower wall, to generate the variation in the liquid temperature across the nanochannel, where k_B is the Boltzmann constant. It is noted that the assumed temperature of the upper and lower wall is only to impose a liquid temperature gradient in a nanochannel. In other words, the assumed wall temperatures could be the other way around. It was safe to assume steady state had been reached after approximately 2 million steps. In all cases we continue a 4 million time step "production run" to determine the temperature profile in the y direction averaged in time and space.

Once the steady temperature profile across the nanochannel is obtained, the degree of thermal slip at the solid surface could be determined. Previous studies generally utilized the hydrodynamic slip length to characterize the velocity slip at the boundary based on the well-known linear Navier model [26,27]. Analogous to the velocity slip, a thermal slip length l_s can be introduced to quantify the thermal slip, which is defined by the linear extrapolation of the fluid temperature profile to the reference boundary, as shown by the red solid line in Fig. 2(b).

It is an important issue where the precise placement of the effective reference boundary is in the determination of thermal slip at a rough surface. And the uncertainty range of thermal slip arises due to the ambiguity of where the reference boundary is placed. It is intuitive that the reference boundary ought to be placed somewhere between the bottom and the top of the asperities, where the bottom and top reference boundaries are both the extreme cases. In the previous investigation of surface roughness effect on boundary velocity slip, the centerline of the surface asperities is generally assumed as the reference boundary [28,29]. However, in order to avoid the arbitrary placement of the reference boundary and fully consider the ambiguity of the reference boundary, the thermal slip length is herein determined with an uncertainty range, in which the reference boundaries at the bottom, centerline, and top of the asperities are all included in this paper. Note that the error bar is applied to describe the uncertainty range, and the thermal slip lengths for the reference boundaries at the bottom, centerline, and top of the asperities are labeled as shown in Fig. 2(c).

IV. RESULTS AND DISCUSSION

A. Temperature distributions

The simulations produced steady-state temperature profiles across the smooth and rough nanochannel, as depicted in Fig. 3. Regardless of whether the nanochannel is smooth or rough, the temperature fields at the central region recover the expected thermal behaviors (i.e., a linear temperature distribution) from heat conduction at the continuum scale as described by Fourier's law. And the deviation of temperature profiles from the linear fashion is observed in the wall-neighboring region where the liquids "feel" the surface energy corrugation.

When compared with an atomically smooth surface, the intrusion of the surface protrusions into liquids increases the amount of energy transfer between the liquids and solid surface and hence results in a small temperature jump at the

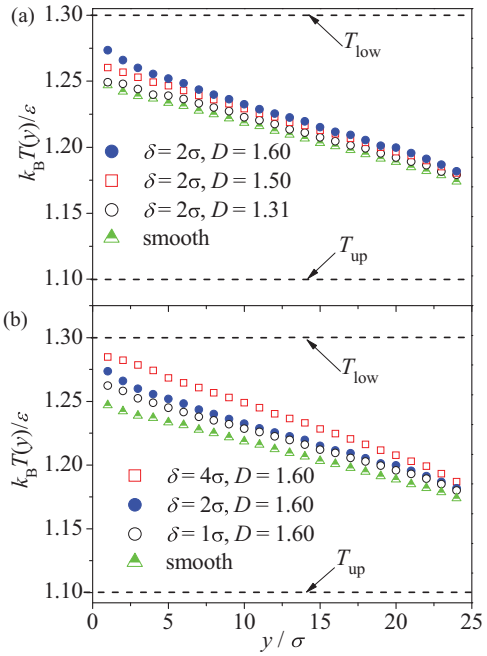

FIG. 3. (Color online) Temperature profiles in smooth and rough nanochannels ($K = 1000\varepsilon\sigma^{-2}$, $\varepsilon_{ls} = 2\varepsilon$).

rough boundary and a large temperature gradient across the nanochannel. In other words, the presence of roughness reduces the thermal slip at the liquid-solid interface. This is also indicated by the figure in that increases in roughness height or fractal dimension can lead to a small thermal slip at the boundary.

So far as the smooth interface is concerned, the temperature profile in the near wall region is not linear. This behavior is attributed to the fact that there are fewer interactions between the liquid molecules in the near wall region than in the core of the liquids. The liquid-solid interaction gradually becomes important when the liquid molecules move closer to the wall. However, in the core of the liquids, the liquid-wall interaction is negligible. Due to varied liquid-solid interaction, the heat transport behavior of liquids confined in the nanochannel is somewhat different for different positions, which finally contributes to the nonlinear distribution of temperature profile perpendicular to the smooth interface.

In addition, as shown in Fig. 3, the thermal slip for the smooth interface is larger near the cold surface than near the hot surface. Owing to low energy, the motion capability of liquids near the cold surface is inferior to those near the hot surface. In this case, there is a weak interaction with a solid wall at low temperatures when the liquid molecules contact with the surface, which contributes to an insufficient energy exchange between the liquid and wall when compared with hot liquid-solid interface.

Seeing that the liquid between the solid surface is not moving, it is interesting to analyze the influence of surface roughness on the diffusion behavior of liquid atoms. Figure 4 illustrates the typical trajectory of liquid atoms in a rough nanochannel. As shown, the surface roughness plays an important role in diffusion behavior of liquid confined in a nanospace. The existence of roughness restricts the motion

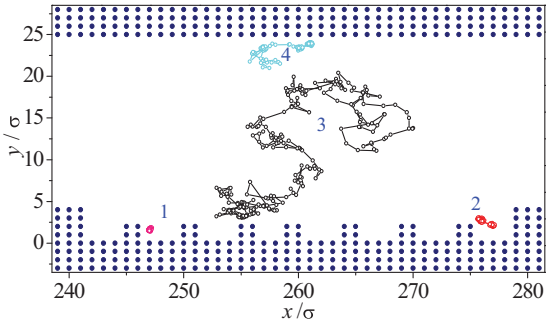

FIG. 4. (Color online) Effect of surface roughness on diffusion behavior of liquid atoms.

capability of liquid in the near wall region. Especially, a few liquid atoms (e.g. No. 1) can become "frozen" by getting stuck to the corner of the solid wall. Note that the stuck "liquid" atoms are still treated as liquid, rather than "solid" when defining the reference boundary in the determination of thermal slip length.

B. Potential energy distributions

To better understand how the thermal slip is affected by roughness height and fractal dimension, as shown in Fig. 3, Fig. 5 presents the local potential energy distributions averaged in time. On the interior of the nanochannels, the potential energy is uniformly distributed. However, in the wall-neighboring region, the potential energy distribution is nonuniform and follows the wall atom placement. The variations of potential energy distributions induced by surface topography are expected to affect the localization and trapping of fluid atoms near a rough wall [18,25]. When compared with a smooth surface, the presence of the roughness expands the low potential energy regions in the adjacent liquids, and the liquid atoms are more likely to be located in these regions. The rough solid wall induces this type of fluid atom behavior in channel layers adjacent to a surface, which extends the time of energy transfer between the solid surface and liquids and finally control the degree of thermal slip at the liquid-solid interface.

Figure 5(a) illustrates the effect of roughness height on the potential energy distributions. As expected, the roughness height plays an important role in the potential energy distribution. The extension of a low potential region, especially in the corner of the valley, is observed with increasing roughness height. This affects the fluid microscopic structure in the near-wall region and gives rise to the modulation of liquid-solid interaction at the boundary. In addition, increases in fractal dimension generate many valleys in the wall accompanied with narrower spacing, which also expands the range of low potential region [see Fig. 5(b)]. For the case of rough surface with $D = 1.60$ and $\delta = 2\sigma$, the valleys of wall are almost in a state of low potential energy. Consequently, even though the wall is of the same statistical roughness height, a surface with larger fractal dimension also introduces more fluid molecules to be trapped inside the valleys and enhance the energy transfer at the boundary.

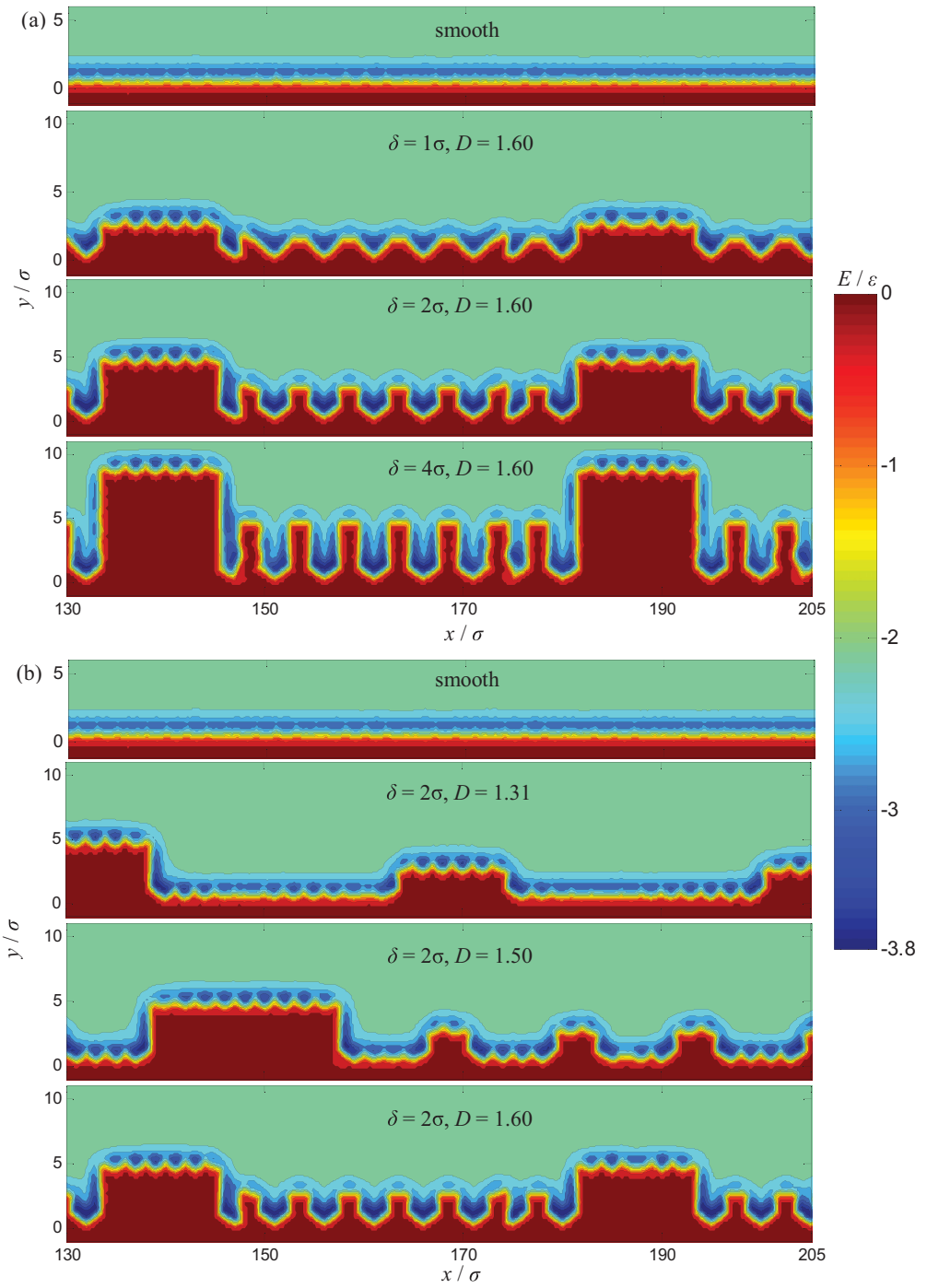

FIG. 5. (Color online) Effect of surface topography on potential energy distributions ($\varepsilon_{ls} = 2\varepsilon$): (a) roughness height and (b) fractal dimension.

C. Effect of solid properties on thermal slip

Considering that 3D systems may exhibit different thermal behavior than 2D systems, Fig. 6 compares the influence of the system dimensionality on the thermal slip for liquids at a smooth solid interface. As shown in the figure, the thermal slip length obtained by the 2D molecular dynamics simulation is different from that obtained by 3D molecular dynamics simulation. This attributes to the different potential gradient in the wall-neighboring region induced by the 3D and 2D solid wall. However, regardless of whether the molecular dynamics simulation is 2D or 3D, the thermal slip length dependence on the liquid-solid interaction is of the same trend.

Figure 7 compares the thermal behaviors at rough and smooth interfaces. Differing from liquid in the bulk, the thermal transport of the liquid at interfaces is affected by the liquid-solid interactions. As seen from the figure, regardless of whether the interface is rough or not, the interfacial interaction energy increases in a linear fashion as related to the strength of the liquid-solid interaction ε_{ls}. The strong interfacial interaction contributes to a sufficient energy exchange between

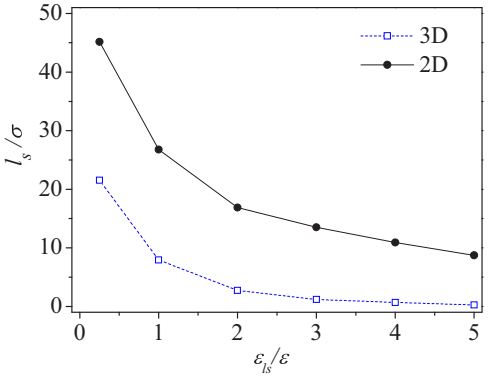

FIG. 6. (Color online) Effect of system dimensionality on the thermal slip ($K = 1000\varepsilon\sigma^{-2}$).

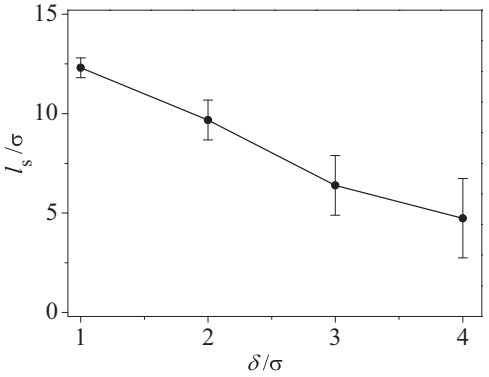

FIG. 8. Effect of roughness height on thermal slip ($D = 1.60$, $\varepsilon_{ls} = 2\varepsilon$).

the liquid and solid surface. As a result, the thermal slip length decreases monotonically with increasing ε_{ls} and finally tends to be a constant. Therefore, it can be concluded that thermal slip occurs for small ε_{ls}, however, the thermal boundary is consistent with a no slip boundary condition for large values of ε_{ls}. In addition, given the strength of the liquid-solid interaction ε_{ls}, the rough surface introduces strong interfacial interaction energy and hence exhibits a relatively small thermal slip when compared with a smooth surface.

The statistical roughness height plays a significant role in the thermal slip, as shown in Fig. 8. The thermal slip length decreases monotonically with increasing statistical roughness height. This behavior can be attributed to the fact that the modulation of the fluid microscopic structure resulting from the increases of roughness height introduces large interfacial interaction energy and contributes to a strong energy exchange between the liquid and solid surface. It is intuitive that a larger roughness height increases the contact area between the solid and the liquid, which results in a better thermal contact and, thus, decrease thermal slip.

Apart from statistical roughness height, the thermal slip is also affected by the topographical irregularity (fractal dimension), as shown in Fig. 9. The walls with a larger fractal dimension yield more frequent variations of the surface profile and provide a larger area for liquids to contact with the solid surface, which greatly enhances the extent to which the liquids feels the corrugation in the solid surface energy (i.e., intensification of the liquid-solid interaction). This effect is essentially the same as increasing statistical roughness height. In addition, increasing fractal dimension has the additional effect of introducing new "corner" sites, which increases the effective interaction strength between the solid and the liquid, thus reducing thermal slip even more.

Previous study on interfacial velocity slip in rough nanochannels indicates that the interfacial velocity slip decreases with increasing statistical roughness height and fractal dimension [16]. Therefore, the role of surface topography on thermal slip at the boundary, including the statistical roughness height and topographical spectrum, is analogous to velocity slip dependence on rough surface [16]. Note that the interfacial velocity slip is determined in a Couette flow geometry with rough surface.

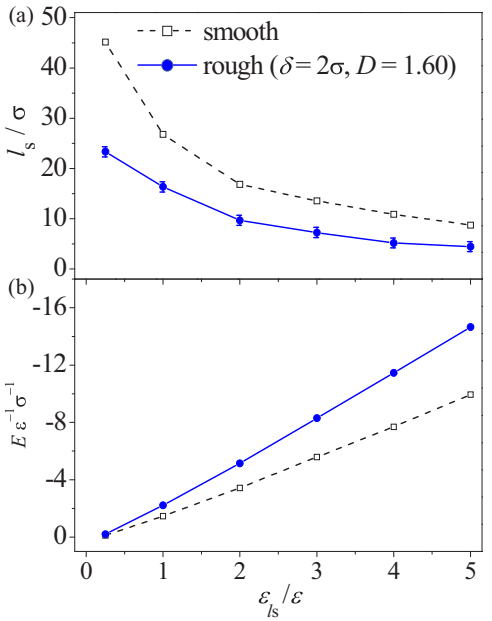

FIG. 7. (Color online) Thermal behaviors at the solid surfaces ($K = 1000\varepsilon\sigma^{-2}$): (a) Thermal slip length and (b) Interfacial interaction energy per unit length.

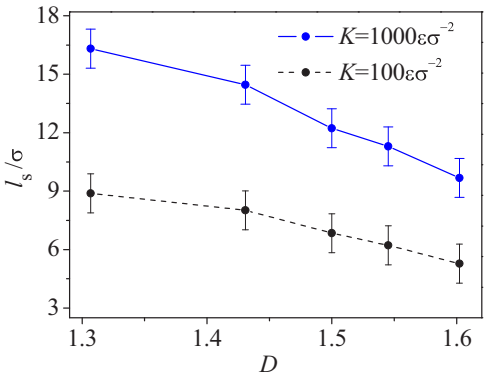

FIG. 9. (Color online) Effect of fractal dimension on thermal slip ($\delta = 2\sigma$, $\varepsilon_{ls} = 2\varepsilon$).

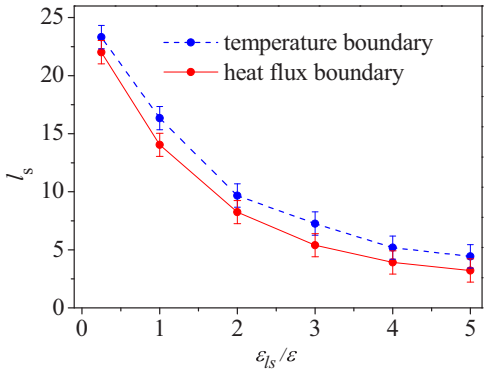

FIG. 10. (Color online) Thermal slip dependency on boundary condition ($D = 1.60$, $\delta = 2\,\sigma$, $K = 1000\varepsilon\sigma^{-2}$).

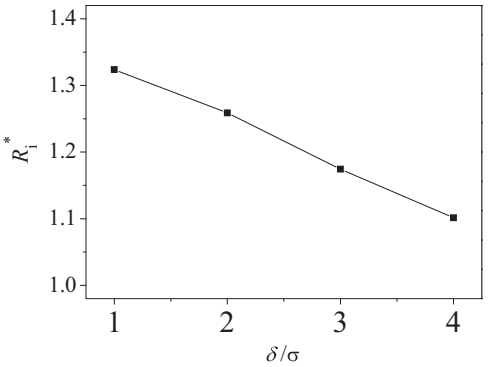

FIG. 11. Effect of roughness height on interfacial thermal resistance ($\varepsilon_{ls} = 2\varepsilon$, $D = 1.55$, $K = 1000\varepsilon\sigma^{-2}$).

The stiffness is also an important physical property of the solid wall, which determines the thermal vibration of wall particles. Previous studies [23] have attempted to correlate the stiffness with interfacial velocity slip and found that decreases in the surface stiffness lead to a small degree of velocity slip. As an analogous behavior, the thermal slip for the liquid at the solid surface is diminished for less stiff surfaces (i.e., smaller value of K), as indicated by Fig. 9. In other words, the trend of thermal slip dependency as affected by surface stiffness is the same as the interfacial velocity slip [23]. The explanation for this phenomenon is that, for the less stiff surfaces, the solid particles are more able to vibrate around their lattice sites, which contributes to a more efficient interfacial momentum and energy transfer at the liquid-solid interface, and consequently results in less slippage in both the velocity and temperature.

Seeing the sensitivity of thermal slip to solid properties, it is important to assess the role of boundary condition on interfacial thermal slip. Two types of boundary conditions are studied, in which one is the constant temperature imposed in the solid, and the other is the constant heat flux imposed on the external surface of the solid. Figure 10 presents the influence of the boundary conditions on thermal slip of liquids at rough solid surfaces. As seen from the figure, the thermal slip degree at the rough solid surface imposed by the constant temperature boundary is larger than that imposed by the heat flux boundary.

D. Effect of surface topography on interfacial thermal resistance

Apart from thermal slip length, the thermal behavior occurring at the rough liquid-solid interface could also be characterized by the interfacial thermal resistance. Therefore, the interfacial thermal resistance is introduced in the current investigation as the evaluation parameter to further verify the role of surface topography on interfacial thermal behavior. The interfacial thermal resistance (R_i) is defined as the ratio between the temperature drop (ΔT) at the liquid-solid interface and the heat flux (q) crossing the interface $R_i = \Delta T/q$. The reduced interfacial thermal resistance is given by

$$R_i^* = R_k \frac{k_B}{\sigma^3}\sqrt{\frac{\varepsilon}{m}}. \tag{5}$$

The thermal resistance at a rough liquid-solid interface is the combination of the Kapitza resistance, directly linked with the solid-liquid interaction, and the constriction resistance due to the presence of the asperities. In order to gain further insight into thermal behavior at the rough liquid-solid interface, the role of surface topography on interfacial thermal resistance are plotted in Figs. 11 and 12. As expected, the surface roughness parameters, including roughness height and fractal dimension, play a significant role in the thermal resistance at the liquid-solid interface. As shown in Fig. 11, a surface with a larger statistical roughness height introduces a smaller thermal resistance at the liquid-solid interface, indicating that the energy transfer between solid and liquid atoms is enhanced at the interface. It is presented by Fig. 12 that, even for the same roughness height, increases in fractal dimension also leads to the reduction of interfacial thermal resistance. Interestingly, the interfacial thermal resistance at a rough liquid-solid interface depends not only on the statistical roughness height, but also on the fractal dimension (i.e., topographical spectrum).

V. CONCLUSION

In the present study we identified and quantified the temperature fields, potential energy distributions, and thermal

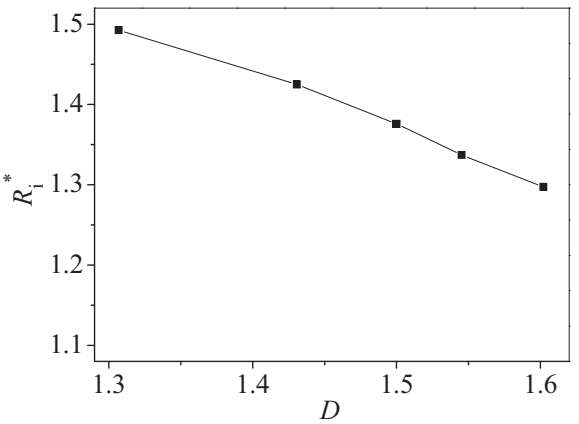

FIG. 12. Effect of fractal dimension on interfacial thermal resistance ($\varepsilon_{ls} = 2\varepsilon$, $\delta = 1\sigma$, $K = 1000\varepsilon\sigma^{-2}$).

slip length in nanochannels incorporating roughness effect as characterized by fractal Cantor structures. These thermal behaviors induced by the statistical roughness height and fractal dimension have been investigated to better understand thermal slip for liquids at rough solid surfaces. In addition, the effects of the liquid-solid interaction, surface stiffness, and boundary condition on thermal slip length are presented. The results indicate that the presence of the roughness expands the low potential energy regions in adjacent liquids, enhances the energy transfer at the liquid-solid interface, and hence decreases the thermal slip at the boundary. A larger roughness height and fractal dimension increases the contact area between the solid and the liquid, which results in a better thermal contact and, thus, decrease thermal slip. In addition, increasing fractal dimension has the additional effect of introducing new corner sites, which increases the effective interaction strength between the solid and the liquid, thus reducing thermal slip even more. Interestingly, even for the same roughness height, a more irregular topography also decreases the interfacial thermal slip and interfacial thermal resistance at liquid-solid interfaces.

ACKNOWLEDGMENT

This work was supported by National Natural Science Foundation of China (Grant No. 51222605), Natural Science Foundation of Jiangsu Province (Grant No. BK2011062), and Research Fund for the Doctoral Program of Higher Education of China (Grant No. 20130092120011).

[1] H. A. Patel, S. Garde, and P. Keblinski, Nano Lett. **5**, 2225 (2005).
[2] M. Cieplak, J. Koplik, and J. R. Banavar, Phys. Rev. Lett. **86**, 803 (2001).
[3] N. Shenogina, R. Godawat, P. Keblinski, and S. Garde, Phys. Rev. Lett. **102**, 156101 (2009).
[4] H. Acharya, N. J. Mozdzierz, P. Keblinski, and S. Garde, Ind. Eng. Chem. Res. **51**, 1767 (2012).
[5] C. Kunert and J. Harting, Phys. Rev. Lett. **99**, 176001 (2007).
[6] B. H. Kim, A. Beskok, and T. Cagin, Microfluid Nanofluid **5**, 551 (2008).
[7] J. L. Barrat and F. Chiaruttini, Mol. Phys. **101**, 1605 (2003).
[8] L. Xue, P. Keblinski, S. R. Phillpot, S. U.-S. Choi, and J. A. Eastman, Int. J. Heat Mass Transfer **47**, 4277 (2004).
[9] Y. Wang and P. Keblinski, Appl. Phys. Lett. **99**, 073112 (2011).
[10] T. L. Warren, A. Majumdar, and D. A. Krajcinovic, ASME J. Appl. Mech. **63**, 47 (1996).
[11] A. Majumdar and C. L. Tien, Wear **136**, 313 (1990).
[12] B. B. Mandelbrot, *The Fractal Geometry of Nature* (Freeman, New York, 1983).
[13] M. Q. Zou, B. M. Yu, J. C. Cai, and P. Xu, ASME J. Heat Transfer **130**, 101301 (2008).
[14] Y. P. Chen, P. P. Fu, C. B. Zhang, and M. H. Shi, Int. J. Heat Fluid Flow **31**, 622 (2010).
[15] Y. P. Chen, C. B. Zhang, M. H. Shi, and G. P. Peterson, Appl. Phys. Lett. **97**, 084101 (2010).
[16] Y. P. Chen, C. B. Zhang, M. H. Shi, and G. P. Peterson, Appl. Phys. Lett. **100**, 074102 (2012).
[17] N. V. Priezjev, J. Chem. Phys **135**, 204704 (2011).
[18] F. D. Sofos, T. E. Karakasidis, and A. Liakopoulos, Phys. Rev. E **79**, 026305 (2009).
[19] J. Sun, W. Wang, and H. S. Wang, Phys. Rev. E **87**, 023020 (2013).
[20] B. H. Kim, A. Beskok, and T. Cagin, J. Chem. Phys. **129**, 174701 (2008).
[21] S. Lepri, R. Livi, and A. Politi, Phys. Rep. **377**, 1 (2003).
[22] M. P. Allen and D. J. Tildesley, *Computer Simulation of Liquids* (Clarendon, Oxford, 1987).
[23] N. Asproulis and D. Drikakis, Phys. Rev. E **81**, 061503 (2010).
[24] N. V. Priezjev, J. Chem. Phys. **127**, 144708 (2007).
[25] F. D. Sofos, T. E. Karakasidis, and A. Liakopoulos, Microfluid Nanofluid **12**, 25 (2012).
[26] S. Granick, Y. X. Zhu, and H. Lee, Nat. Mater. **2**, 221 (2003).
[27] P. A. Thompson and S. M. Troian, Nature (London) **389**, 360 (1997).
[28] N. V. Priezjev and S. M. Troian, J. Fluid Mech. **554**, 25 (2006).
[29] A. Niavarani and N. V. Priezjev, J. Chem. Phys. **129**, 144902 (2008).